Langmuir
Article
pubs.acs.org/Langmuir

Print-and-Peel Fabricated Passive Micromixers

Marlon S. Thomas, Joseph M. Clift, Brent Millare, and Valentine I. Vullev*

Department of Bioengineering, University of California, Riverside, California 92521

Received August 4, 2009. Revised Manuscript Received November 17, 2009

Advection driven mixing is essential for microfluidics and poses challenges to the design of microdevices. Force transducers or complex channel configurations provide means for, respectively, active or passive disrupting of laminar flows and for homogenizing the composing fluids. Print-and-peel (PAP) is a nonlithographic fabrication technique that involves direct printing of masters for molding polymer components of microdevices. PAP, hence, allows for facile and expedient preparation of microfluidic devices, without requiring access to specialized microfabrication facilities. We utilized PAP for fabrication of microfluidic devices capable of turning, expanding, and contracting microflows. We examined the mixing capabilities of these devices under flow conditions of small Reynolds numbers (0.2−20) and large Péclet numbers (260−26 000), under which advection is the dominant mode of mass transfer. We focused on mixing channels with arched shapes and examined the dependence of the mixing performance on the turns and the expansions along the direction of the microflows. Three-dimensional expansion and contraction, along with an increase in the modes of twisting of the laminar currents, improved the quality of mixing. The simplicity in the described fabrication of the investigated passive micromixers makes PAP an attractive alternative for expedient device prototyping.

Introduction

This article describes a comparative study of the performance of nonlithographically fabricated micromixers. Using print-and-peel (PAP) approaches, we fabricated a series of microfluidic (μFL) devices, in which channels with round cross sections served as mixing chambers. We tested the performance of these PAP-fabricated micromixers at relatively small Reynolds numbers, *Re*, ranging between about 0.2 and 20. Expectedly, the addition of curvatures in the direction of the fluid flows improved the mixing performance of the PAP-fabricated devices.

Microfluidics has gained significance as an interdisciplinary technology with a broad range of applications in chemistry, biology, and physics.[1−14] Laminar flows are prevalent in μFL devices due to the relatively small Reynolds numbers characteristic of the small cross sections of the channels.[15] Such laminar microflows have proven immensely beneficial for applications, such as membraneless fuel cells[16−18] and optical waveguiding,[7,19,20] which require well-defined interfaces between miscible liquids. For other types of microfluidics applications, involving "lab-on-a-chip" analytical and sensing techniques, achieving fast and efficient mixing in submicroliter volumes is imperative.[21−26] Fast and efficient mixing in biosensors and bioanalytical microdevices, for example, not only assures speed and quality in the overall device performance, but also allows for direct monitoring of the dynamics of chemical and biochemical processes with subsecond resolution.[27]

Decreasing the cross sections of the channels and slowing down the fluid flows will allow for diffusion-driven homogenizing of miscible liquids at small Reynolds numbers and at small Péclet numbers.[23,28−30] For small-Péclet-number conditions, however, relatively long time spans, exceeding the diffusion time constants, are required. For example, the characteristic diffusion times, τ_D, for 15 kDa globular proteins in aqueous media, are about 23 s, 90 s, and 350 s for diffusion lengths, l, of 50 μm, 100 μm, and 200 μm, respectively

$$\tau_D = \frac{l^2}{D} \quad (1)$$

*E-mail: vullev@ucr.edu.

(1) Chen, H.; Fan, Z. H. *Electrophoresis* **2009**, *30*, 758–765.
(2) Abdelgawad, M.; Wheeler, A. R. *Adv. Mater.* **2009**, *21*, 920–925.
(3) van Noort, D.; Ong, S. M.; Zhang, C.; Zhang, S.; Arooz, T.; Yu, H. *Biotechnol. Prog.* **2009**, *25*, 52–60.
(4) Leng, J.; Salmon, J.-B. *Lab Chip* **2009**, *9*, 24–34.
(5) Sorger, P. K. *Nat. Biotechnol.* **2008**, *26*, 1345–1346.
(6) Sia, S. K.; Kricka, L. J. *Lab Chip* **2008**, *8*, 1982–1983.
(7) Psaltis, D.; Quake, S. R.; Yang, C. *Nature* **2006**, *442*, 381–386.
(8) Paguirigan, A. L.; Beebe, D. J. *BioEssays* **2008**, *30*, 811–821.
(9) Walker, G. M.; Zeringue, H. C.; Beebe, D. J. *Lab Chip* **2004**, *4*, 91–97.
(10) Moorthy, J.; Beebe, D. J. *Anal. Chem.* **2003**, *75*, 292A–301A.
(11) Beebe, D. J.; Mensing, G. A.; Walker, G. M. *Annu. Rev. Biomed. Eng.* **2002**, *4*, 261–286.
(12) Atencia, J.; Beebe, D. J. *Nature* **2005**, *437*, 648–655.
(13) Weibel, D. B.; Garstecki, P.; Whitesides, G. M. *Curr. Opin. Neurobiol.* **2005**, *15*, 560–567.
(14) Mehta, G.; Lee, J.; Cha, W.; Tung, Y.-C.; Linderman, J. J.; Takayama, S. *Anal. Chem.* **2009**, *81*, 3714–3722.
(15) Brody, J. P.; Yager, P.; Goldstein, R. E.; Austin, R. H. *Biophys. J.* **1996**, *71*, 3430–3441.
(16) Abruna, H. D.; Matsumoto, F.; Cohen, J. L.; Jin, J.; Roychowdhury, C.; Prochaska, M.; van Dover, R. B.; DiSalvo, F. J.; Kiya, Y.; Henderson, J. C.; Hutchison, G. R. *Bull. Chem. Soc. Jpn.* **2007**, *80*, 1843–1855.
(17) Ferrigno, R.; Stroock, A. D.; Clark, T. D.; Mayer, M.; Whitesides, G. M. *J. Am. Chem. Soc.* **2002**, *124*, 12930–12931.
(18) Jayashree, R. S.; Gancs, L.; Choban, E. R.; Primak, A.; Natarajan, D.; Markoski, L. J.; Kenis, P. J. A. *J. Am. Chem. Soc.* **2005**, *127*, 16758–16759.
(19) Vezenov, D. V.; Mayers, B. T.; Conroy, R. S.; Whitesides, G. M.; Snee, P. T.; Chan, Y.; Nocera, D. G.; Bawendi, M. G. *J. Am. Chem. Soc.* **2005**, *127*, 8952–8953.
(20) Mayers, B. T.; Vezenov, D. V.; Vullev, V. I.; Whitesides, G. M. *Anal. Chem.* **2005**, *77*, 1310–1316.
(21) Stone, H. A.; Stroock, A. D.; Ajdari, A. *Ann. Rev. Fluid Mech.* **2004**, *36*, 381–411.
(22) Hessel, V.; Loewe, H.; Schoenfeld, F. *Chem. Eng. Sci.* **2005**, *60*, 2479–2501.
(23) Locascio, L. E. *Anal. Bioanal. Chem.* **2004**, *379*, 325–327.
(24) Ottino, J. M.; Wiggins, S. *Science* **2004**, *305*, 485–486.
(25) Campbell, C. J.; Grzybowski, B. A. *Philos. Trans., Ser. A* **2004**, *362*, 1069–1086.
(26) Stroock, A. D.; Dertinger, S. K. W.; Ajdari, A.; Mezit, I.; Stone, H. A.; Whitesides, G. M. *Science* **2002**, *295*, 647–651.
(27) Song, H.; Chen, D. L.; Ismagilov, R. F. *Angew. Chem., Int. Ed,* **2006**, *45*, 7336–7356.
(28) The Péclet number represents the ratio between the advection and diffusion contributions to mass transfer.
(29) Nauman, E. B.; Nigam, A. *Chem. Eng. Technol.* **2004**, *27*, 293–296.
(30) Hattori, K.; Sugiura, S.; Kanamori, T. *Lab Chip* **2009**, *9*, 1763–1772.

where D is the diffusion coefficient, and for lysozyme (MW = 14.5 kDa) and myoglobin (MW = 16.9 kDa) in aqueous media, $D = 1.1 \times 10^{-6}$ cm^2 s^{-1}.[31]

The long time periods, along with the relatively small amounts of material that can be processed, make diffusion-dominated mixing impractical for a large number of microfluidic applications. Introducing advection to low-Reynolds-number microflows, on the other hand, significantly accelerates their mixing.

Advection-dominated mixing at low Reynolds numbers and at high Péclet numbers, therefore, is essential for μFL devices. Folding currents with miscible liquids within one another decreases the diffusion lengths and, hence, considerably decreases the characteristic diffusion times. In microdevices, such effects are achieved via incorporating active or passive micromixers as components of the devices. Active micromixers employ external oscillating forces for disturbing the laminar flows,[25,32−34] while passive micromixers rely on complex channel geometries to achieve the desired advection.[22,26,35] Chaotic micromixers comprising asymmetric "herringbone"-shaped grooves on the floors of microchannels, for example, provide complete mixing at small Reynolds and large Péclet numbers, e.g., $Re < 100$ and $Pe = 20\,000$.[26] Utilizing droplets, introduced in microchannels as "plugs" of immiscible fluids with volumes of femtoliters to microliters, presents an alternative for achieving millisecond-mixing times via advection and short diffusion length scales.[24,27] The complexity of such passive micromixers, however, places challenging requirements on their fabrication, which often involves multistep procedures.

Recently, we demonstrated the utility of print-and-peel for fabrication of μFL sensors.[36−38] Computer-aided design (CAD) patterns were directly printed onto smooth substrates to produce masters with positive relief features of two-dimensional (2D) channel configurations. Placing three-dimensional (3D) elements on printed masters, allowed us to fabricate curved off-plane channels that acted as mixers in continuous-flow μFL sensors in a single polymer-molding step (see Supporting Information).[36−38] This PAP nonlithographic methodology offers simplicity and expedience in prototyping microdevices with various complexities.[36−41]

Khine et al. further explored PAP[41−43] and fabricated micromixers that performed efficiently at Reynolds numbers between 10 and 55.[43] No 3D elements were employed, however, and the fabrication involved preparing four polymer slabs and stacking them over one another with precise alignment.[43]

By employing solely 3D elements, without CAD patterns, Ghatak et al. demonstrated the fabrication of complex patterns of channels within polymer slabs.[44−47] Using this approach, they fabricated in a single molding step microchannels with round cross sections and with helical grooves along the channel walls.[44,45] This channel geometry forced advection currents and mixing at a wide range of Reynolds numbers.[45]

As mentioned above, PAP allowed us to fabricate a μFL sensor equipped with two inlet channels:[36] (1) a reagent inlet channel for a continuous flow of a luminogenic indicator solution and (2) a thin injection channel through which small volumes of analyte are introduced. Through a relatively wide channel, following the merging of the reagent and injection channels, the laminar flow was carried into an arched mixing chamber/channel prior to emission detection.[36] We showed the mixing performance of these devices under pulsatile regime; i.e., we injected small volumes of colored aqueous solution (e.g., 1 to 40 μL) and observed its homogenization with water continuously flowing through the reagent inlet channel.[36]

Employing a series of PAP-fabricated μFL devices, herein, we tested the features that govern the efficiency of the PAP-fabricated off-plane arched micromixers.[36,38] Our findings revealed that, in addition to the geometry of the micromixers, the direction of introducing the laminar flows into the mixers plays a crucial role for the quality of mixing.

Results and Discussion

PAP Fabrication. Using a solid-ink printer,[37,40,48] the CAD patterns were printed on overhead transparency films to produce positive-relief features of 2D channel networks. To complete the masters for molding the polymer components of the devices, onto the printed features we adhered 3D elements that formed the mixing arched channel as well as the inlet and outlet connecting channels. We cast polydimethylsiloxane (PDMS) over the masters. Having allowed the elastomer to cure, we removed it from the printouts and pulled the 3D elements from the bulk of the PDMS slabs to produce the polymer components of the devices. Following oxygen-plasma activation of the surfaces of the device components,[49] we permanently attached the PDMS slabs to glass slides to complete the microdevices (see Supporting Information).

As we and others have demonstrated, solid ink printers reproduce smoother features in comparison with the LaserJets with compatible resolution.[36−38,40,48] The channels from the CAD-printed features had large aspect ratios: they were about 10 to 15 μm high and more than 250 μm wide.[38]

Mixing. We examined the mixing performance of the devices under continuous-flow conditions. Colored and colorless aqueous solutions were allowed to continuously flow through both inlet channels. Before entering the mixing arched channel, the colored and colorless liquids were clearly separated in a laminar fashion, after the arch, the color was distributed across the channel width (Figure 1a).

Gray-scale analysis of the image revealed near complete mixing for flow rates from 4 to 400 μL/min. We plotted the

(31) Liu, M.-K.; Li, P.; Giddings, J. C. *Protein Sci.* **1993**, *2*, 1520–1531.
(32) Ryu, K. S.; Shaikh, K.; Goluch, E.; Fan, Z.; Liu, C. *Lab Chip* **2004**, *4*, 608–613.
(33) Liu, R. H.; Yang, J.; Pindera, M. Z.; Athavale, M.; Grodzinski, P. *Lab Chip* **2002**, *2*, 151–157.
(34) Oddy, M. H.; Santiago, J. G.; Mikkelsen, J. C. *Anal. Chem.* **2001**, *73*, 5822–5832.
(35) Villermaux, E.; Stroock, A. D.; Stone, H. A. *Phys. Rev. E* **2008**, *77*, 015301.
(36) Vullev, V. I.; Wan, J.; Heinrich, V.; Landsman, P.; Bower, P. E.; Xia, B.; Millare, B.; Jones, G., II *J. Am. Chem. Soc.* **2006**, *128*, 16062–16072.
(37) Hong, C.; Bao, D.; Thomas, M. S.; Clift, J. M.; Vullev, V. I. *Langmuir* **2008**, *24*, 8439–8442.
(38) Thomas, M. S.; Millare, B.; Clift, J. M.; Bao, D.; Hong, C.; Vullev, V. I. *Ann. Biomed. Eng.*, in press.
(39) Coltro, W. K. T.; Piccin, E.; Fracassi da Silva, J. A.; Lucio do Lago, C.; Carrilho, E. *Lab Chip* **2007**, *7*, 931–934.
(40) Kaigala, G. V.; Ho, S.; Penterman, R.; Backhouse, C. J. *Lab Chip* **2007**, *7*, 384–387.
(41) Chen, C.-S.; Breslauer, D. N.; Luna, J. I.; Grimes, A.; Chin, W.-c.; Lee, L. P.; Khine, M. *Lab Chip* **2008**, *8*, 622–624.
(42) Grimes, A.; Breslauer, D. N.; Long, M.; Pegan, J.; Lee, L. P.; Khine, M. *Lab Chip* **2008**, *8*, 170–172.
(43) Long, M.; Sprague, M. A.; Grimes, A. A.; Rich, B. D.; Khine, M. *Appl. Phys. Lett.* **2009**, *94*, 133501/133501–133501/133503.
(44) Verma, M. K. S.; Majumder, A.; Ghatak, A. *Langmuir* **2006**, *22*, 10291–10295.
(45) Verma, M. K. S.; Ganneboyina, S. R.; Rakshith, R, V.; Ghatak, A. *Langmuir* **2008**, *24*, 2248–2251.
(46) Majumder, A.; Ghatak, A.; Sharma, A. *Science* **2007**, *318*, 258–261.
(47) Arul, E. P.; Ghatak, A. *Langmuir* **2009**, *25*, 611–617.
(48) Wang, W.; Zhao, S.; Pan, T. *Lab Chip* **2009**, *9*, 1133–1137.
(49) Millare, B.; Thomas, M.; Ferreira, A.; Xu, H.; Holesinger, M.; Vullev, V. I. *Langmuir* **2008**, *24*, 13218–13224.

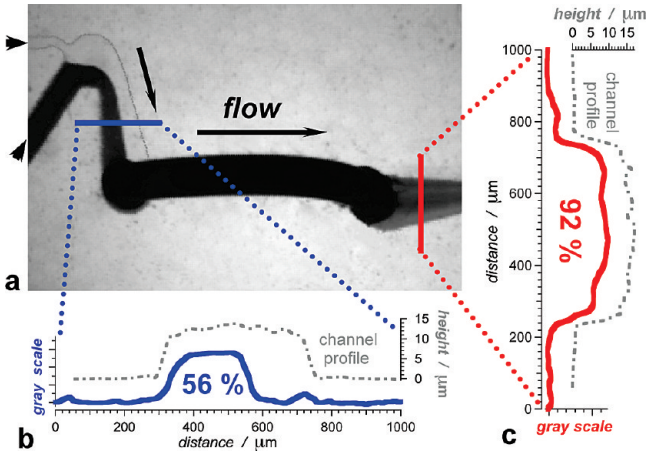

Figure 1. Mixing at low-Reynolds-number regime in a continuous-flow device with an arched round channel (Scheme 1a). (a) Transmission optical microscopy image of the continuous-flow mixing device (see Supporting Information).[36] Water was allowed to flow through the injection (upper) inlet channel, and aqueous solution of crystal violet (20 mM) was flowed through the reagent (lower) inlet channel. Each of the two liquids was introduced at 20 μL/min flow rate; hence, the total flow rate through the arched channel and through the channels leading to and away from the arch, was 40 μL/min. (b) Distribution of the gray-scale intensity across the channel before the arch. The solid blue line represents the gray scale. For comparison, the gray dashed−dotted line represents the cross section of the channel (obtained from profilometry data). For convenient visualization, the profilometry traces (Figure 1a) across the negative-relief features on the PDMS slab were inverted (i.e., multiplied by −1) and represented as "height", rather than "depth". For the gray-scale distribution ratio, the gray-scale curve and the profile trace were normalized to height of unity and baseline of zero, and numerically integrated. Dividing the integral of the gray scale by the integral of the profile trace yielded the gray-scale distribution ratio, 53 ± 8%, as averaged from three measurements. (c) Distribution of the gray-scale intensity across the channel after the arch with the corresponding gray-scale distribution ratio, 94 ± 6%. The solid red line represents the gray-scale distribution, and the dashed−dotted line represents the cross section of the channel.

relative gray scale of each pixel vs the pixel coordinate along a strip crossing the analyzed channel, as we have previously demonstrated.[36] The cross section of the channels, obtained from profilometry data, allowed us to estimate the expected shapes of the gray-scale profiles across the channels widths. We estimated the extent of distribution of the color across the channel as a ratio between the integrals of the normalized gray-scale profiles obtained from the images and of the channel-height profiles obtained from the profilometery data.

Homogeneous distribution of color across the channel, due to complete mixing, for example, led to integral ratios close to 100%. For the channels carrying the laminar flows before the mixing arch, the color-distribution ratios were around 50%, i.e., ranging from about 40% to about 60% (Figure 1b). For this analysis, we assumed laminar illumination along the heights of the flat CAD-patterned channels, which for channel heights less than ~20 μm and small angular aperture used for these images is an acceptable approximation.

The described gray-scale analysis readily reveals lateral mixing patterns, i.e., along the width and the length of the channels. This image-based analysis, however, is not truly informative about possible vertical color inhomogeneities, i.e., along the height of the channels. The aspect ratios between the widths and the heights of the printer-patterned channels are between 40 and 80 (see Supporting Information). Because the characteristic diffusion time is proportional to the square of the diffusion length (eq 1), the lateral characteristic diffusion time across the channel widths is more than 3 orders of magnitude larger than the characteristic diffusion time along the vertical cross sections of the channels. For these particular aspect ratios, therefore, the efficiency of homogenizing the laminar flow patterns across the channel widths, adequately revealed by the image gray-scale analysis, is the limiting process for efficient mixing.

The color-distribution ratio across the channel after the mixing arch was an indication for the extent of mixing. Color-distribution ratios above 90% indicated practically complete mixing and below 60% indicated no mixing. We observed adequately complete mixing for the tested device with the original configuration (Figure 1c).[36]

Role of the Arched Shape for the Mixing Process. The mixing arched channels were situated on planes orthogonal to the plane of the CAD patterned channels.[36] The radius of the curvature of the arch was about 1.3 mm. The arched channels had circular cross sections with 420 μm diameter, making them about 30 times larger than the cross-sectional areas of the CAD-patterned channels leading to and from the arch termini. For flow rates of 4, 40, and 400 μL/min, therefore, the Reynolds numbers, *Re*, or the fluid flows inside the arched channels were, respectively, 0.2, 2 and 20, which were smaller than the values of Re for the same flow rates in the flat CAD-patterned channels.

$$Re = \frac{2rV}{\nu} = \frac{2\rho Q}{\pi\mu r} \tag{2}$$

where ν and μ are the kinematic and dynamic viscosities, respectively; ρ is the fluid density; V is the average fluid velocity; and Q is the flow rate through a round channel with a radius r.

The diffusion coefficient, D, of the used dye, crystal violet, in water ($D = 7.55 \times 10^{-6}$ cm^2 s^{-1}),[50] yielded relatively large Péclet numbers, *Pe*, for the arched channel

$$Pe = Re\,Sc = \frac{2Q}{\pi rD} \tag{3}$$

where *Sc* was the Schmidt number, and *Pe* ranged from 260 to 2.6×10^4 for flow rates from 4 to 400 μL/min, respectively. Such large Péclet numbers suggested that the observed mixing was advection dominated.

The conclusions drawn from the large values of the Péclet numbers were also supported by the comparison between the diffusion and residence times of the dye in the arched channel. The characteristic diffusion time across the cross section of the arched channel was about 2 min (eq 1). The residence times for a dye molecule in the arched channel were 9, 0.9, and 0.09 s for the used flow rates of 4, 40, and 400 μL/min, respectively. Because the residence times for all flow rates were considerably shorter than the characteristic diffusion time, diffusion by itself could not have produced the observed mixing. Therefore, the employed channel geometry caused sufficient advection to fold the laminar currents into one another, shortening the diffusion lengths and the characteristic diffusion times.

(50) Mouquin, H.; Cathcart, W. H. *J. Am. Chem. Soc.* **1935**, *57*, 1791–1794.

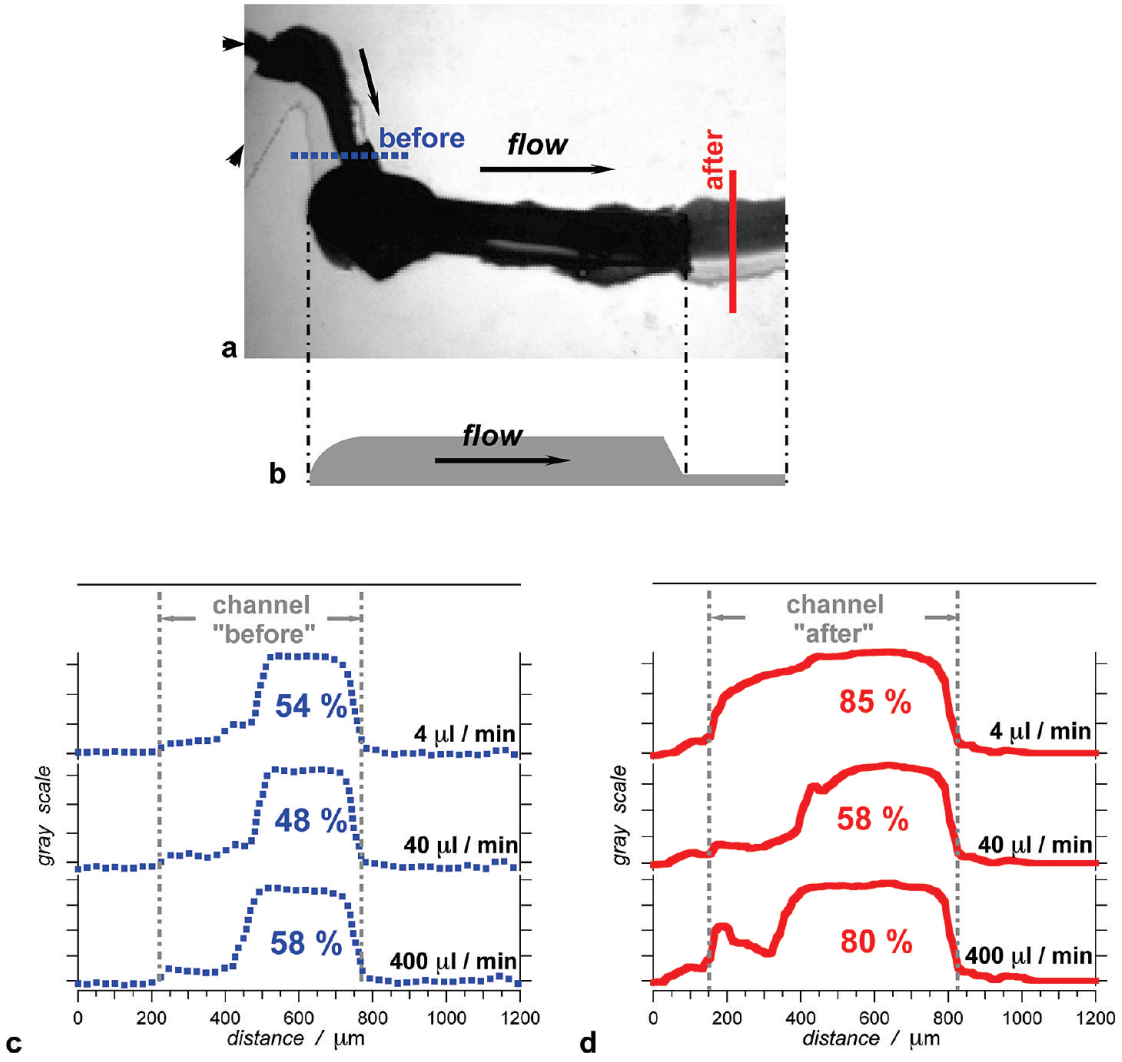

Figure 2. Performance of a device with a straight channel, instead of an arch (Scheme 1b). (a) Transmission optical microscopy image of the device. Water and aqueous solution of crystal violet (20 mM) were allowed to flow, respectively, through the reagent (lower) and the injection (upper) inlet channel. Each of the two liquids was introduced at 200 μL/min flow rate; hence, the total flow rate through the device after merging the two flows was 400 μL/min. (b) Schematic representation of the side view of the device straight and exit channels. (c) Distribution of the gray-scale intensity across the channel before entering the large-cross-section channel for different flow rates, with the corresponding gray-scale distribution ratios (error between 5% and 8%). (d) Distribution of the gray-scale intensity across the channel after exiting the large-cross-section channel for different flow rates, with the corresponding gray-scale distribution ratios (error between 7% and 12%). The dashed−dotted gray lines in (c) and (d) represent the channel boundaries.

The Dean number, κ, representing the ratio between viscous and centrifugal forces acting on curved fluid flows[51−57]

$$\kappa = Re\sqrt{\frac{r}{R}} \qquad (4)$$

where R is the radius of the arch, and r is the radius of the cross section of the arched channel.[57]

The values of the Dean number ranged between 0.08 and 8 for the employed flow rates through the arched channels with 1.3 mm radius of the arch. Such small values of κ for 4 and 40 μL/min suggested that the origin of the mixing at these flow rates was not secondary fluid currents caused by centrifugal forces resultant from the curved direction of the flows traveling along the arched channel.

We examined the contribution of the arched geometry by testing the mixing by a device, in which the round-cross-section channel with identical dimensions was straight, rather than arched (Figure 2). When we used a straight large-cross-section channel, situated onto the plane of the CAD-patterned channels, the quality of mixing deteriorated (Figure 2d). The lack of mixing was especially pronounced at the intermediate flow rate we used, i.e., at 40 μL/min. It should be noted, however, that at 40 μL/min the boundary line between the colored and colorless currents shifted toward the colorless solution (Figure 2c,d), i.e., toward the exterior of the sharp right-angle turn that the fluids undertook entering the wide channel (Scheme 1b).

(51) Berger, S. A.; Talbot, L.; Yao, L.-S. *Ann. Rev. Fluid Mech.* **1983**, *15*, 461–512.
(52) Verkaik, A. C.; Beulen, B. W. A. M. M.; Bogaerds, A. C. B.; Rutten, M. C. M.; van de Vosse, F. N. *Phys. Fluids* **2009**, *21*, 023602/023601–023602/023613.
(53) Mouza, A. A.; Patsa, C. M.; Schönfeld, F. *Chem. Eng. Res. Des.* **2008**, *86*, 1128–1134.
(54) Schönfeld, F.; Hessel, V.; Hofmann, C. *Lab Chip* **2004**, *4*, 65–69.
(55) Kim, S.; Lee, S. J. *Exp. Fluids* **2009**, *46*, 255–264.
(56) Jiang, F.; Drese, K. S.; Hardt, S.; Küpper, M.; Schönfeld, F. *AIChE J.* **2004**, *50*, 2297–2305.
(57) The Dean number has also been defined as $K = 2^{1/2}\kappa$, and as $K = \kappa^2/2$. In eq 4, for example, the diameter, d, instead the radius, r, of the channel has been used.

An increase in the flow rate to 400 μL/min further increased the shift of the boundary line between the colored and colorless current (Figure 2c,d). For 4 μL/min, on the other hand, the gray color was gradually distributed into the "colorless side" of the channel (Figure 2c,d).

By itself, the right-angle turn of the flow upon entering into the wide channel was not sufficient for the observed partial mixing at the investigated flow rates (Figure 2). For devices with the same CAD-patterned geometry, but no wide channel added, we did not observe even partial mixing at 4 to 400 μL/min (Figure 3b). Furthermore, two-dimensional expansion of the fluid only within the CAD plane did not cause any mixing (Figure 3c,d). These findings demonstrate the importance of the rapid three-dimensional expansion of the fluid for creating chaotic advection essential for efficient mixing.

The radius of the arch curvature was, indeed, too large to expect chaotic advection resultant from the turn of the flows through the arched channel. The difference in the mixing results for the arched and the straight channel (Figures 1 and 2), however, indicated that the quality of mixing depended on the direction of the flow after expending into the wide, round channels. While for the straight channel (Figure 2) the overall flow direction was along the CAD plane of the device, for the arched channel (Figure 1) the liquid flowed 90° "upward" off the plane, turned in the arch, and flowed back to the same plane to take another sharp right-angle turn to exit the arched channel. Apparently, these three turns in the flow, and hence the arched geometry of the channel, were key for efficient mixing.

Direction of Entering the Arched Channel. The laminar flows entered the arched channel perpendicular to the plane of the arch and turned 90° "upward" (Scheme 1a). Therefore, the boundary plane, separating the laminar flows, was perpendicular to the plane of the arch. Should incompletely mixed liquid remained, the plane separating these unmixed currents would be orthogonal to the CAD-patterned plane of the device and orthogonal to the plane of the arch (Scheme 1a). The liquid flowing "downward" from the arch would sharply turn into the 10-μm-high exit channel. The boundary plane, separating the laminar currents, would be parallel to the floor of the high-aspect-ratio exit channel, forcing the remaining unmixed liquid

Scheme 1. Direction of Flows through Devices with Different Configuration

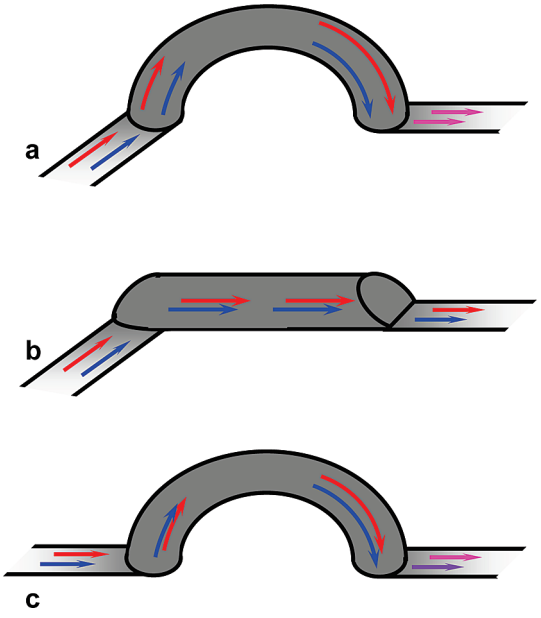

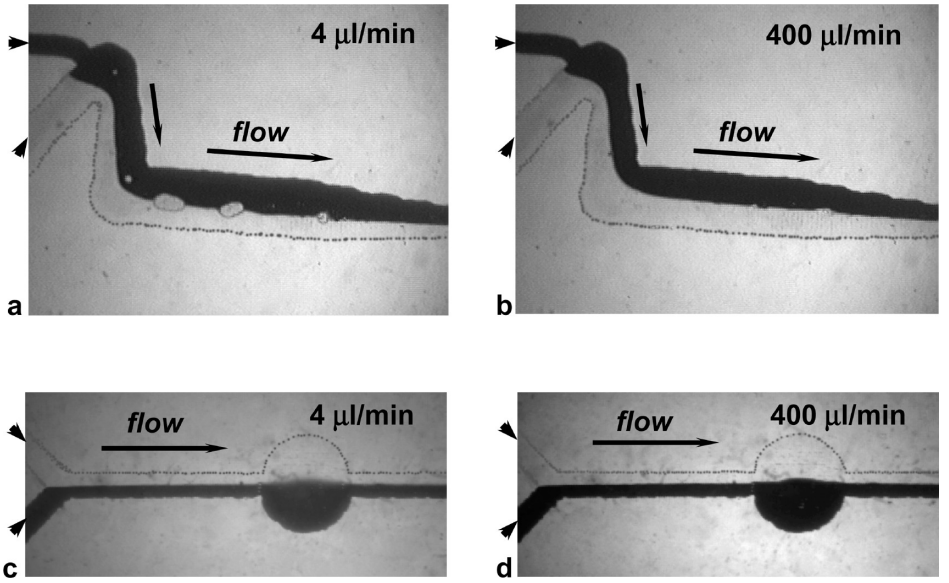

Figure 3. Transmission optical microscopic images of devices comprising solely flat CAD-patterned channels. The images show the flow patterns through the devices at different flow rates. (a,b) Device with the geometry of the continuous-flow μFL sensor (see Supporting Information),[36] in which the mixing arch was replaced with CAD-patterned flat channel. Water and aqueous solution of crystal violet (20 mM) were introduced through, respectively, the reagent (lower) and the injection (upper) inlet channel at combined flow rates of (a) 4 μL/min, and (b) 400 μL/min. The Reynolds numbers for these channels were about an order of magnitude smaller than the Reynolds numbers for the large-cross-section channels (Figure 2, Scheme 1b) for the same flow rates. (c,d) Y-junction device (see Supporting Information), in which the arched channels was replaced with a CAD-patterned circle. Water and aqueous solution of crystal violet (20 mM) were flowed through, respectively, the upper and the lower inlet channel of the Y junction to form two-component laminar currents with combined flow rates of (c) 4 μL/min and (d) 400 μL/min. For improved visualization, the borders of the channels, filled with the colorless liquid, are outlined with gray dotted lines.

currents to fold over one another within the confined channel height.

In contrast, for the straight channel (Figure 2, Scheme 1b), the boundary plane between the colored and colorless laminarly flowing liquids did not turn or twist. The boundary plane remained parallel to the direction of the exiting channel and perpendicular to the CAD-patterned plane of the device (Scheme 1b). Therefore, forcing the flow into the small-height exit channel would cause folding of liquids only of the same color into one another. Overall, such liquid current patterns would yield incomplete mixing, which was consistent with the observed results (Figure 2).

To examine the merit of this somewhat simplified view of the contribution of the direction of the current turns to the quality of mixing, we fabricated and tested devices in which the entry and exit channels lay on the same line. The flow in such a device also experienced a sharp right-angle turn "upward", followed by a curved turn of the arched channel, and another sharp right-angle turn toward the exit channel. Unlike in the original setup (Scheme 1a), however, the boundary plane between the laminar-flowing colored and colorless liquids remained parallel to the plane of the arch and orthogonal to the CAD-patterned plane of the device (Scheme 1c).

The performance of such Y-junction devices with smooth, arched channels revealed partial mixing at 40 and 400 μL/min (Figure 4). The presence of partial mixing and the lack of a well-defined boundary line between the colored and colorless solutions in the channel after the arch suggested advection processes folding the laminar currents into one another as the fluid passed in, through, and out of the arched channel. This contrast with the results from the device with a straight channel (Figure 2) further demonstrated the importance of the arched geometry for the mixing process.

A comparison between the performance of the original device (Figure 1)[36] and the Y-junction device (Figure 4) revealed inferior mixing when the entry and exit channels were along the same line (Figures 1c and 4b). Therefore, the direction at which the laminar flows entered the arched mixing channels was determinant for the extent of observed mixing.

Importance of Twists and Turns. Our findings showed the key importance of the manner in which the laminar flows were turned so that the boundary planes, separating the laminarly moving liquids, were twisted to cause folding of currents and decreasing of the diffusion lengths. We demonstrated that the original device configuration provides efficient mixing under continuous-flow conditions due to (1) the arched shape of mixing channel, (2) the expanded cross-section of the mixing channel, and (3) the direction of introducing the laminar flow into the mixing channel (Figure 1, Scheme 1a).

The performance of universally applicable micromixers, however, should not depend on the exact device configuration and on the direction of the inflow. To decouple the quality of performance from the direction of the laminar inflows, we explored additional advection modes within the mixing arch. Helical grooves along the walls of the arched channels (Figure 5b) allowed us to introduce an alternative mode of twisting of the liquid flows in the mixing channels.

Arch-channel mixers with helical grooves along their walls installed in Y-junction devices resulted in complete mixing for all tested flow rates (Figure 5c). In comparison with the smooth arched channels (Figure 4), the arch with helical grooves produced superior mixing for the tested flow rates (Figure 5c).

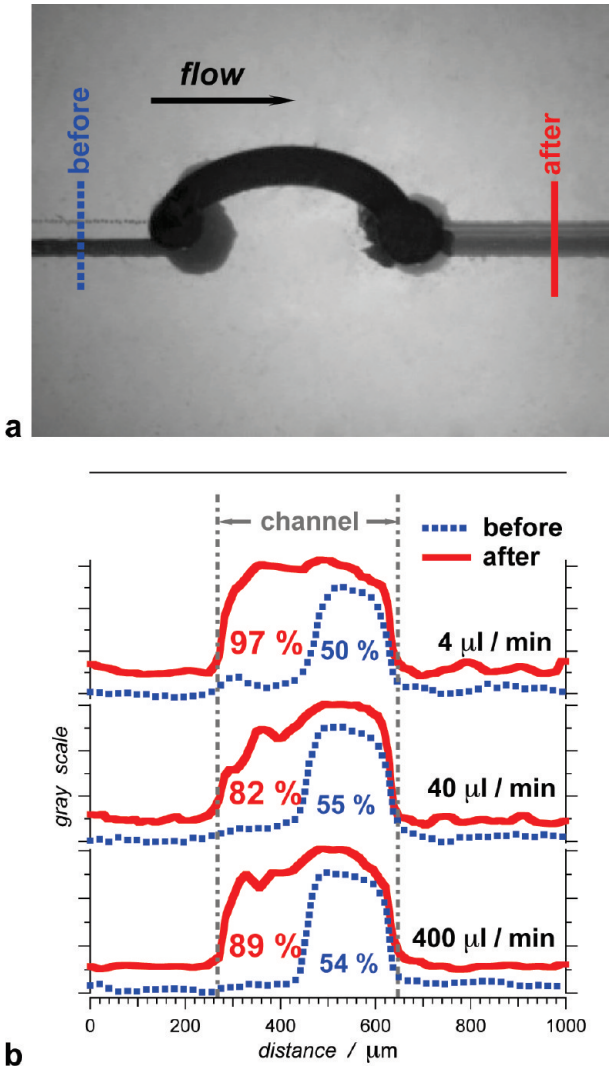

Figure 4. Performance of a Y-junction device comprising an arched channel with circular cross section (Scheme 1c). (a) Transmission optical microscopy image of the arched section of the device (see Supporting Information). Laminar currents of water and aqueous solution of crystal violet (20 mM) are flowed into the arch at 400 μL/min flow rate. (b) Distribution of the gray-scale intensity across the channel before (blue dotted lines) and after (red solid lines) the arch (at different flow rates) with the corresponding gray-scale distribution ratios (error between 4% and 8%). The dashed−dotted gray lines represent the channel boundaries.

The helical grooves along the walls of the mixing channels add an additional curvature in the direction of the flow. As defined in eq 4, κ cannot exceed *Re*. Although the addition of the spiral grooves allows for maximizing the Dean number for the employed flow conditions, the values for κ are still relatively small due to the small values of *Re*. Furthermore, the Dean number provides dimensionless evaluation of two-dimensional flows, and its application to three-dimensional flow geometries, i.e., an arch of a helix, is not necessarily an appropriate approximation. In fact, Ghatak et al. observed efficient mixing in helical channels at apparent Dean numbers smaller than ~10,[45] which is in agreement with our findings. Apparently, the shear between the laminar flows twisted in the helically grooved, arched channels provides the advection essential for efficient mixing.

Dimensionless flow characteristics, such as Dean number (eq 4), indeed, provide guidance for optimizing the design of micromixers.[53−56] For flow conditions at relatively small Dean

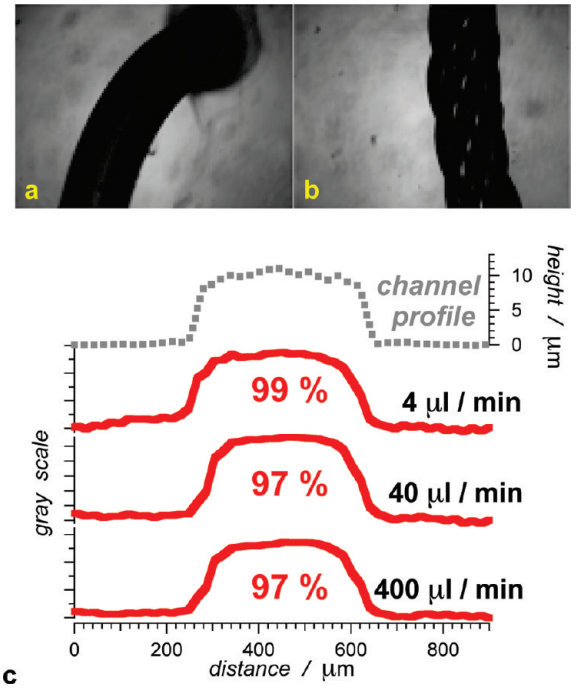

Figure 5. Performance of a Y-junction device comprising a round, arched channel with helical grooves along the walls. Transmission optical microscopy images of (a) a section of an arched channel with smooth walls and (b) a section of an arched channel with four grooves helically winding along the circular wall. (c) Distribution of the gray-scale intensity across the channel after the arch with grooved walls. The solid red lines represent the gray-scale intensity across the channel with the corresponding gray-scale distribution ratios (at different flow rates; error less than 5%), and the dotted gray line represents the cross section of the channel (from profilometry data).

numbers, however, we observed mixing comparable with the mixing from, for example, meandering microdevices at intermediate and high κ.[53,56] Therefore, such dimensionless analysis cannot encompass all the processes responsible for the mixing that we observed for these PAP-fabricated devices.

The Dean numbers we calculated are descriptive of the flows moving through the arched channels and not of the flows at the points of entry and exit of the arch. Furthermore, the arch-of-a-helix geometry (Figure 5b) adds another level of complexity that presents a challenge for analysis using solely dimensionless quantities. Regardless of the small apparent Dean numbers, our findings confirm that the irregularities, involving twists, sharp turns, and expansions and contractions of the flows, prevalently provide the advection essential for fast and complete mixing at small Reynolds and large Péclet numbers.

Conclusions

Print-and-peel (PAP) allowed us to expediently and facilely fabricate a range of microfluidic device with potential mixing capabilities. The tested geometries of the arched channels provided not only turns in the flow direction, but also expansion and contraction of the liquid currents at the entry and the exit of the arch. Such flow geometries proved essential for achieving efficient mixing. Additional flow twists, caused by helically grooved channel walls, resulted into close-to-ideally complete mixing. Mixing at low Reynolds numbers and large Péclet numbers is an important design challenge for microfluidic devices. PAP has the potential for making such designs achievable without access to specialized microfabrication facilities.

Acknowledgment. This work was supported by the U.S. Department of Education and the U. C. Regents Faculty Development Award. We extend our gratitude to Prof. Victor G. J. Rodgers for the helpful discussions on the mass-transport phenomena.

Supporting Information Available: Experimental details. This material is available free of charge via the Internet at http://pubs.acs.org.